

Synthesis, Anti-tubercular Activity and Molecular Docking of Novel Metformin incorporated 4,5-Diaryl Imidazole Derivatives

Rajasekhar Kumarachari Komarla*, Hemalatha Aramati, Mayandigari Guruvareddy, Kodadhavadi Mohammad Ishaqulla, Balaji Saran, Mopuru Hemanth Yadav

*Rajasekhar Kumarachari Komarla

¹*Department of Pharmaceutical Chemistry, Sri Padmavathi School of Pharmacy, Tiruchanur, Tirupati-517503, Andhra Pradesh, India.

Corresponding author mail id: komarla.research@gmail.com

Abstract

The targeted compounds were synthesized by mixing 2-hydroxy-1,2-diarylethanoate with metformin in the presence of ethanol and screened for anti-tubercular activity of novel diaryl imidazole derivatives and predict their affinity against *Mycobacterium tuberculosis* GlmU. The synthesized imidazole derivatives were determined using *Mycobacterium tuberculosis* H37RV strain. The binding affinity of the synthesized compounds to GlmU was determined using MOE docking simulation. Compounds **5b-5e** have showed a very interesting anti-tubercular activity having 0.8 µg/mL MIC value. The other compounds also showed a promising MIC of 6.25 µg/mL or less against *Mycobacterium tuberculosis* H37RV strain. The synthesized compounds have also showed high binding affinity to GlmU. The catalytic amino acid residues of GlmU-His374, Asn397 and Ala391, were found to interact with the synthesized imidazole derivatives.

Key words: Anti-tubercular activity, Imidazole, GlmU, Molecular docking

Introduction

The annual number of TB deaths is falling globally, but not fast enough to reach the 2020 milestone of a 35% reduction between 2015 and 2020. The COVID-19 pandemic threatens to reverse recent progress in reducing the global burden of TB disease. The global number of TB deaths could increase by around 0.2 - 0.4 million in 2020 alone. An increase in frequency and distribution of multi-drug resistant TB (MDR-TB) and extensive drug resistant TB (XDR-TB) throughout the world is considered as one of the contributing reasons for TB death. A total of 480,000 cases of MDR-TB were estimated to occur in 2014, of which an estimate 190,000 deaths occurred. An estimated 9.7% of people with MDR-TB have XDR-TB¹. To make the conditions even worse, totally drug resistant TB (TDR-TB) has emerged over several countries, no effective treatment options exist for those patients as the strain is resistant to all available anti-TB drug²⁻¹⁰. Those reports necessitated an increased medicinal chemists' effort in the discovery and development of novel anti-tubercular agents.

Many imidazole based drugs have been extensively used to treat various types of diseases, including but not limited to cancer; fungal, bacterial and protozoal infections and hyperacidity¹¹⁻¹³. Various researches have established the anti-tubercular activity of imidazole based drugs¹⁴⁻¹⁸. Research on imidazole based drugs as anti-tubercular agents is very much alive. Nitroimidazopyran PA-824 is an investigational drug at the advanced stage of clinical trial against both replicating and latent *Mycobacterium tuberculosis* (*Mtb*)¹⁹⁻²⁰. This inspired numerous researchers to put a lot of effort in search of novel imidazole based anti-tubercular drugs. In continuation of our interest in the synthesis of nitrogen heterocyclics^{21,22}, herein, an efficient synthesis of 2,4,5-trisubstituted imidazoles has been developed by a condensation of various substituted benzoin and metformin (N-C-N fragment

guanidine equivalent) in refluxing ethanol under mild reaction conditions in good yields. As an important output of this work, metformin is introduced as a novel and efficient N-C-N fragment guanidine equivalent in the synthesis of substituted imidazoles.

The synthesized molecules were docked against GlmU enzyme of *Mtb*(GlmU^{Mtb}). Docking simulation was done in order to predict the binding affinity of the synthesized imidazole derivatives against GlmU^{Mtb}. This will demonstrate if there exist a relation between affinity to GlmU^{Mtb} and Minimum Inhibitory Concentration (MIC) for imidazole based anti-tubercular agents. The docking may generate useful information on the structure based design of imidazole based anti-GlmU^{Mtb} agents.

GlmU is a bifunctional enzyme which possess acetyltransferase and uridyltransferase activities. In the acetyl transfer reaction, which is catalyzed by the C-terminal domain of GlmU, the acetyl group from Acetyl-CoA is transferred to the amine group of glucosamine 1-phosphate (GlcN-1-P) to produce N-acetylglucosamine 1-phosphate (GlcNAc-1-P). GlcNAc-1-P then diffuses to the N-terminal domain to form UDP-N-acetylglucosamine 1-phosphate (UDP-GlcNAc) by the transfer of UMP from UTP. UDP-GlcNAc is important for synthesizing lipopolysaccharide and peptidoglycan components of the cell wall²³⁻²⁵. UDP-GlcNAc is essential in both eukaryotes and prokaryotes, although each use a different biosynthetic pathway. Moreover, the acetyltransferase domain of GlmU^{Mtb} and the eukaryotic analogue are structurally distinct and have difference in substrate specificity. GlmU^{Mtb} is unique and essential for optimal growth of *Mtb*²⁶. This has produced a spotlight on the acetyltransferase activity of GlmU^{Mtb} as an excellent target for developing selective anti-tubercular drugs.

The biologically active form of GlmU is a trimer form, where the C-terminal domain active site is formed by the involvement of all the three monomer units with contribution from left handed alpha helices of two subunits, insertion loop of one subunit and C-terminal extension of the third subunit[Figure 1]. As a result, it is crucial that the macromolecule should be in trimeric form for docking simulation studies²⁷.

Experimental

General synthetic procedure of 2-(1,1-dimethyl guanidiny)-4,5-diaryl imidazoles: 5a–5j

Aqueous sodium hydroxide solution (0.4 g, 5mL) and aromatic aldehyde (**2a-2j**) were added to a solution of thiamine hydrochloride **1** (1.75 g, 0.005 M, 5mL) in ethanol (95%, 5mL). The mixture was heated gently on a water bath for 90 min, which was cooled to room temperature and then placed in ice bath to induce crystallization. The solid obtained was filtered, washed several times with water, dried and re-crystallized with ethanol to 2-hydroxy-1,2-diaryl ethanoate (**3a-3j**)[Figure 2]. Completion of the reaction was determined by TLC using cyclohexane: ethyl acetate (2:1) mixture as mobile phase.

A mixture of 2-hydroxy-1,2-diaryl ethanone (0.01 mol) and metformin **4** (0.01 mol) was mixed in ethanol and then refluxed for 4 hrs. The reaction mixture was cooled and triturated with crushed ice. The product obtained was filtered, washed thoroughly with small portions of cold water, dried and re-crystallized from ethanol to get 2-(1,1-dimethyl guanidiny)-4,5-diaryl imidazole(**5a- 5j**). The purity of the synthesized derivatives was verified using TLC on silica gel G-plates and cyclohexane: ethyl acetate (2:1) mixture as mobile phase. The spots on the plates were visualized using UV chamber.

Compounds **5a**, **5b**, **5c**, **5d**, **5e**, **5f**, **5g**, **5h**, **5i** and **5j** were synthesized by adopting the above synthetic procedures and varying the aromatic substituents (**3a-3j**).

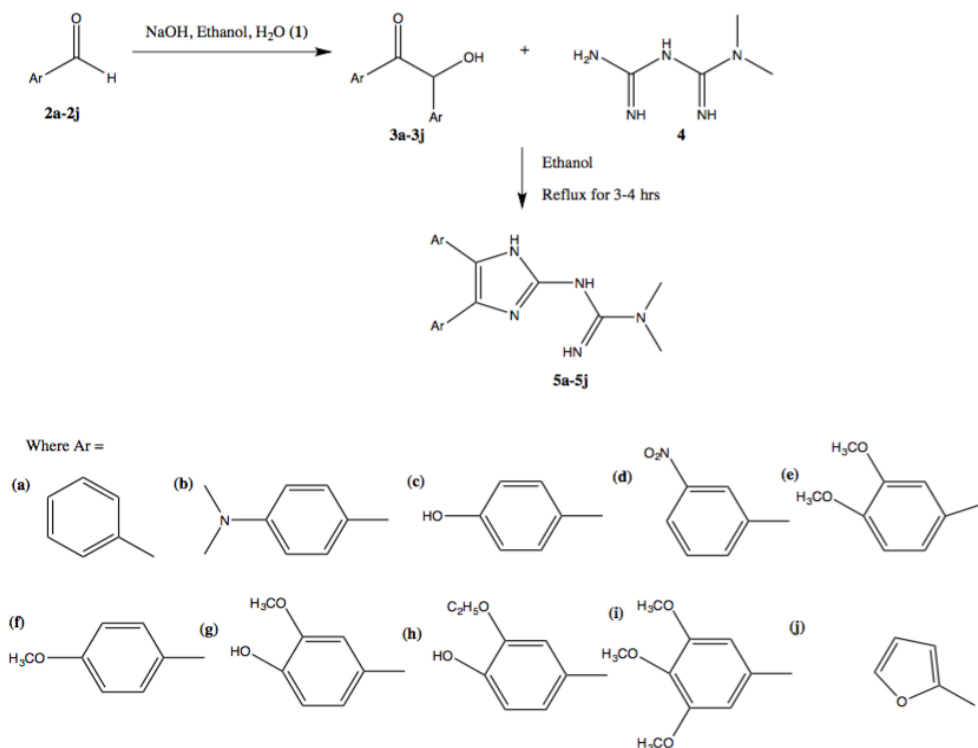


Figure 1; General synthetic route for 2-(1,1-dimethyl guanidiny)-4,5-diaryl imidazole derivatives

The IUPAC and spectra details of the synthesized imidazole derivatives

2-(N,N-dimethyl guanidiny)-4,5-diphenyl imidazole [5a]

Yield, 87%: mp 162-165⁰C; FT-IR(KBr): 1078(3⁰N), 1680(C=N), 1317(2⁰N), 1182(ArC-N-C), 1577(N-H) cm⁻¹; ¹HNMR (CDCl₃): δ 2.5(s, 6H, CH₃), 4.6(m, 2H, NH), 5.5(s, 1H, =NH), 7.2(m, 10H, Ar) ppm; MS (m/z, %): 306.42(M⁺); Anal. Cal. for C₁₈H₁₉N₅: C:70.80, H:6.27, N:22.93. Found: C:70.25, H:6.50, N:22.66.

2-(N,N-dimethyl guanidiny)-4,5-bis[4-(dimethylamino)phenyl] imidazole [5b]

Yield, 85%: mp 84-87⁰C; FT-IR (KBr): 1063(3⁰N), 1689(C=N), 1336(2⁰N), 1178(ArC-N-C), 1591(N-H) cm⁻¹; ¹HNMR (CDCl₃): δ 2.5(s, 6H, CH₃), 3.0(m, 12H, CH₃), 4.5(m, 2H, NH), 5.0(s, 1H, =NH), 6.5(m, 8H, Ar) ppm; MS (m/z, %): 392.85(M⁺); Anal. Cal. for C₂₂H₂₉N₇: C:67.49, H:7.47, N:25.04. Found: C:66.30, H:7.49, N:25.75.

2-(N,N-dimethyl guanidiny)-4,5-bis[4-hydroxyl phenyl] imidazole [5c]

Yield, 86.6%: mp 145-148⁰C; FT-IR (KBr): 1072(3⁰N), 1665(C=N), 1315(2⁰N), 1182(ArC-N-C), 1219(C-O), 3572(O-H), 1596(N-H) cm⁻¹; ¹HNMR (DMSO): δ 2.48(s, 6H, CH₃), 4.2(m, 2H, NH), 5.5(s, 1H, =NH), 2.1(s, 2H, OH), 6.9(m, 8H, Ar) ppm; MS (m/z, %): 338.79(M⁺); Anal. Cal. for C₁₈H₁₉N₅O₂: C:64.08, H:5.68, N:20.76, O:9.48. Found: C:64.02, H:5.72, N:20.79, O:9.47.

2-(N,N-dimethyl guanidiny)-4,5 –bis[3-nitro phenyl] imidazole [5d]

Yield, 81.4%: mp 244-247⁰C; FT-IR (KBr): 1107(3⁰N), 1624(C=N), 1327(2⁰N), 1170(ArC-N-C), 582(NO₂), 1566(N-H) cm⁻¹; ¹HNMR (CDCl₃): δ 2.2(s, 6H, CH₃), 4.0(m, 2H, NH), 5.2(s,

1H, =NH), 7.8(m, 8H, Ar) ppm; MS (m/z, %) :396.91(M⁺); Anal. Cal. for C₁₈H₁₇N₇O₄: C:54.68, H:4.33, N:24.80, O:16.19. Found: C:54.76, H:4.26, N:24.77, O:16.21.

2-(N,N-dimethyl guanidiny)-4,5-bis[3,4-dimethoxy phenyl] imidazole [5e]

Yield, 83%: mp 246-249⁰C; FT-IR (KBr): (3⁰N), 1649(C=N), 1281(2⁰N), 1027(C-O-C), 1188(ArC-N-C), 1590(N-H),2812(C-O) cm⁻¹; ¹HNMR (DMSO): δ 2.4(s, 6H, CH₃), 3.3(s, 12H, OCH₃), 3.8(m, 2H, NH), 4.9(s, 1H, =NH), 6.8(m, 6H, Ar) ppm; MS (m/z, %): 426.73(M⁺); Anal. Cal. for C₂₂H₂₇N₅O₄: C:62.10, H:6.40, N:16.46, O:15.04. Found: C:62.55, H:6.27, N:16.55, O:14.63.

2-(N,N-dimethyl guanidiny)-4,5-bis[4-methoxy phenyl] imidazole [5f]

Yield, 78%: mp 118-120⁰C; FT-IR (KBr): 1094(3⁰N), 1601(C=N), 1304(2⁰N), 1046(C-O-C), 576(NO₂), 1172(ArC-N-C), 1574(N-H) cm⁻¹; ¹HNMR (DMSO): δ 2.8(s, 6H, CH₃), 3.7(s, 6H, OCH₃), 4.2(m, 2H, NH), 5.1(s, 1H, =NH), 7.1(m, 8H, Ar) ppm; MS (m/z, %): 366.86(M⁺); Anal. Cal. for C₂₀H₂₃N₅O₂: C:65.73, H:6.34, N:19.16, O:8.77. Found: C:65.79, H:6.20, N:19.20, O:8.81.

2-(N,N-dimethyl guanidiny)-4,5-bis[4-hydroxy-3-methoxy phenyl] imidazole [5g]

Yield, 78%: mp 90-94⁰C; FT-IR(KBr):1102(3⁰N), 1664(C=N), 1318(2⁰N), 1239(C-O), 1178(ArC-N-C), 3548(O-H), 1589(N-H) cm⁻¹; ¹HNMR (DMSO): δ 2.5(s,6H,CH₃), 3.6(s, 6H,OCH₃), 4.2(m, 2H, NH), 5.1(s, 1H, =NH), 1.8(s, 2H, OH), 6.9(m, 6H, Ar) ppm; MS (m/z, %): 398.98(M⁺); Anal. Cal. for C₂₀H₂₃N₅O₄: C:60.44, H:5.83, N:17.62, O:16.11. Found: C:60.42, H:5.53, N:17.89, O:16.16.

2-(N,N-dimethylguanidiny)-4,5-bis[3-ethoxy-4-hydroxy phenyl] imidazole [5h]

Yield, 84%: mp 242-245⁰C; FT-IR(KBr):1077(3⁰N), 1635(C=N), 1382(2⁰N), 1223(C-O), 1187(ArC-N-C), 3551(O-H), 1598(N-H) cm⁻¹; ¹HNMR (DMSO): δ 2.6(s,6H,CH₃), 3.7(m, 4H, OCH₂), 1.2(s, 6H,CH₃), 4.2(m, 2H, NH), 5.4(s, 1H, =NH), 2.1(s, 2H, OH), 7.2(m, 6H, Ar) ppm; MS (m/z, %) :426.67(M⁺); Anal. Cal. for C₂₂H₂₇N₅O₄: C:62.10, H:6.40, N:16.46, O:15.04. Found: C:62.33, H:6.32, N:16.44, O:14.91.

2-(N,N-dimethyl guanidiny)-4,5-bis[3,4,5-trimethoxy phenyl] imidazole [5i]

Yield, 85.5%: mp 160-165⁰C; FT-IR(KBr):1116(3⁰N), 1654(C=N), 1340(2⁰N), 1217(C-O), 1183(ArC-N-C), 1582(N-H) cm⁻¹; ¹HNMR (DMSO): δ 2.5(s, 6H, CH₃), 3.6(s, 18H, OCH₃), 4.0(m, 2H, NH), 5.2(s, 1H, =NH), 6.9(m, 4H, Ar) ppm; MS (m/z, %) :486.73(M⁺); Anal. Cal. for C₂₄H₃₁N₅O₆: C:59.37, H:6.44, N:14.42, O:19.77. Found: C:58.82, H:6.32, N:16.33, O:18.53.

2-(N,N-dimethylguanidiny)-4-(furan-2-yl)-5-(furan-3-yl) imidazole [5j]

Yield, 87%: mp 180-184⁰C; FT-IR(KBr):1137(3⁰N), 1671(C=N), 1358(2⁰N), 1183(ArC-N-C), 1560(N-H) cm⁻¹; ¹HNMR (DMSO): δ 2.6(s, 6H, CH₃), 4.3(m, 2H, NH), 5.5(s, 1H, =NH), 7.2(m, 6H, Ar) ppm; MS (m/z, %): 286.81(M⁺); Anal. Cal. for C₁₄H₁₅N₅O₂: C:58.94, H:5.30, N:24.55, O:11.21. Found: C:58.52, H:5.23, N:24.83, O:11.42.

Anti-tubercular activity

The imidazole derivatives were evaluated for anti-tubercular activity using Microplate Alamar Blue Assay (MABA) method. Accordingly, each derivative was screened against *Mtb*

H37RV strain using streptomycin, pyrazinamide and ciprofloxacin as standard drugs at concentrations of 6.25 µg/mL, 3.125 µg/mL and 3.125 µg/mL respectively.

During MABA method, 200µL of sterile deionized water was added to all outer perimeter wells of sterile 96 wells plate to minimize evaporation of the medium during incubation. 100 µL of the MB 7H9 broth was added to the 96 wells plate and serial dilution of derivatives was made directly on plate. The final drug concentrations of the derivatives tested were 0.2, 0.4, 0.8, 1.6, 3.125, 6.25, 12.5, 25, 50 and 100 µg/mL. Plates were sealed with parafilm and incubated at 37°C for five days. After this time, 25µL of freshly prepared 1:1 mixture of Alamar blue reagent and 10% Tween 80 was added to the plate and then incubated for 24 hrs. A blue color in the well was interpreted as no bacterial growth, and pink color was scored as growth. MIC, which is the concentration required to inhibit 90% of the standardized bacterial inoculums, was defined as the lowest drug concentration which prevented the color change from blue to pink²⁸.

Molecular docking

The predicted trimeric biological assembly of the crystal structure of GlmU^{Mtb} in complex with GlcN-1-P was retrieved from protein data bank in Europe (PDB ID 3ST8)²⁹. The model was refined using ModRefiner online tool and the resulting model was validated by producing the Ramachandran plot. The LigX panel was used for the preparation of the protein, which provides an automated process for structural correction, protonation, tethering and minimization stages of structure preparation. The site finder panel, on the other hand, was used to identify the binding site of the target protein.

The 2D chemical structures were imported into Molecular operating environment (MOE) database, which was visually inspected for bonding patterns and washed in order to correct any structure drawing error. The ligands were minimized using MMFF94x force field, during which hydrogen atom was added and atomic partial charges were calculated.

Docking simulation was performed using MOE docking panel. MOE generated several binding poses using a triangle matcher placement method. The scores assigned to each generated poses by the placement method were re-scored using London dG. Thirty poses were retained from the placement stage, which were refined using MMFF94x force field. The final refined poses were then re-scored using GBVI/WSA dG force field based scoring function and the pose with the highest final score was selected as the binding affinity value of the ligand.

Results and Discussion

A facile scheme has been developed to synthesize the targeted compounds (**5a-5j**). They were synthesized by mixing 2-hydroxy-1,2-diarylethanoate (**3a-3j**) with metformin (**4**) in the presence of ethanol. The percentage yield can be referred from the spectra details.

The proposed scheme was very effective as it led to the synthesis of compounds which are in conformity with what was envisioned. Structural confirmation was done depending on the spectral data from Fourier Transform Infrared spectroscopy (FT-IR), Proton Nuclear Magnetic Resonance (¹H NMR) spectroscopy and Mass Spectrometry (MS). In addition, analytical data were also used for structural confirmation. In all cases the compounds were obtained in pure form, which were further purified by recrystallization from ethanol.

Anti-tubercular activity

The synthesized imidazole derivatives were evaluated for anti-tubercular activity according to MABA method [Table 1]. It is very interesting to note that synthesized compounds **5b-5e**

exhibited marked anti-tubercular activity at a concentration of 0.8 $\mu\text{g/mL}$. The rest of the compounds, **5a** and **5f-5j**, also exhibited significant anti-tubercular activity at concentrations ranging from 1.6 to 6.25 $\mu\text{g/mL}$.

Compared to compound **5a**, compounds **5b-5e** contains additional hydrogen bond accepting substituent, which may be the reason for the approximately eight times more anti-tubercular activity observed with those compounds. On the other hand, increasing the size of the meta alkoxy substituent was found to increase the anti-tubercular activity of compound **5h** compared to compound **5g**. However, the use of methoxy group at both meta positions may be detrimental to activity, which can be noted from the approximately eight times less activity of compound **5i** compared to compound **5e**. The equal MIC value of compound **5a** and compound **5j** showed that furanyl group can be used as a bioisostere analogue of phenyl group when it comes to the anti-tubercular activity of imidazole derivatives.

Table 1: The anti-tubercular activity (MIC values and the binding affinities to GlmU) of the synthesized imidazole derivatives

Compounds	<i>Mtb</i> H ₃₇ RV MIC ($\mu\text{g/mL}$)	Binding affinity (Kcal/mol) from MOE
5a	6.25	-6.42
5b	0.8	-7.51
5c	0.8	-6.36
5d	0.8	-7.35
5e	0.8	-7.29
5f	1.6	-6.85
5g	6.25	-7.27
5h	3.125	-8.01
5i	6.25	-7.86
5j	6.25	-6.27

Molecular docking

Ramachandran plot, which is a commonly used indicator of quality of a protein structure, of the refined macromolecule was obtained using RAMPAGE³⁰. Accordingly, the percentage of amino acid residues in the favored region and in allowed region was 98.1% and 2.9% respectively. In addition, the number of amino acid residues in the outlier region of the Ramachandran plot was none.

An induced fit docking simulation was performed using MOE³¹. The binding site for docking was determined using the site finder panel of MOE. Accordingly, the binding pocket composed of Trp560 and Arg465 from chain A; Arg344, Lys362, Tyr377, Val394, Phe395, Val396, Asn397, Tyr398, Asp399, Gly400, Lys403 and Val421 from chain B; and Lys354, Lys371, Pro373, His374, Asn388, Ile389, Gly390, Ala391, Arg413, Thr414, Gly415, Ser416, Tyr431, Thr432, Gly433, Ala434 and Leu447 from chain C was selected [Figure 4]. This pocket was chosen because the catalytic mechanism of GlmU was reported to involve His374, Asn397 and Ala391. Accordingly, the amino group of GlcN-1-P will produce a nucleophilic attack on the carbonyl group of acetyl-coA. His374 and Asn397 bind with the amino group of GlcN-1-P so that the nucleophilic reaction will shift forward. Ala391, on the other hand, facilitate the reaction by stabilizing the intermediate through hydrogen bonding interaction.

The type of intermolecular interactions between the amino acids in the active site of GlmU and the ligands is given in Table 2. All compounds had created at least one hydrogen bond

interaction, except compounds **5b** and compound **5e**. All of the synthesized imidazole derivatives have created either hydrogen or hydrophobic interaction with HisB374 and AsnA397, the two most important amino acids for the acetyl transfer reaction catalyzed by GlmU. With the exception of compounds **5c** and **5d**, all compounds showed intermolecular interaction with AlaB391.

Similar to the anti-tubercular evaluation, the docking simulation showed that the affinity of compound **5h** was higher than compound **5g**. This increased affinity to GlmU may be attributed to the replacement of methoxy substituent at meta position with an ethoxy substituent.

Table 2: Summary of the type of interactions and the amino acids interacting with the synthesized imidazole derivatives

Ligands	HB interactions	Hydrophobic interactions
Compound 5a	LysB371 arene-cation	ArgA344, TyrA377, ValA394, PheA395, Val A396, AsnA397, TyrA398, LysA403, LysB354, ProB373, HisB374, AsnB388, GlyB390, AlaB391, ArgB413, SerB416
Compound 5b		TyrA342, ArgA344, GluA360, ValA394, PheA395, AsnA397, TyrA398, LysA403, LysB354, LysB371, ProB373, HisB374, AsnB388, GlyB390, AlaB391, TyrB398, ArgB413, SerB416
Compound 5c	ArgA344, TyrA398 H-arene	ArgA344, TyrA377, AsnA397, TyrA398, LysA403, GlyB369, LysB371, HisB374, TyrB386, SerB387, AsnB388, ArgB413
Compound 5d	ArgA344, LysA362, TyrA377, AsnA397, LysA403	TyrA398, LysB354, GlyB369, LysB371, ProB373, HisB374, SerB387, AsnB388, ArgB413
Compound 5e		TyrA342, ArgA344, TyrA377, ValA394, PheA395, ValA396, AsnA397, TyrA398, LysA403, LysB354, LysB371, ProB373, HisB374, AsnB388, GlyB390, AlaB391, ArgB413
Compound 5f	TyrA398 H-arene	ArgA344, TyrA377, PheA395, ValA396, AsnA397, TyrA398, LysA403, LysB354, LysB371, ProB373, HisB374, AsnB388, IleB389, GlyB390, AlaB391, SerB416
Compound 5g	TyrA398 H-arene	ArgA344, GluA360, TyrA377, ValA394, PheA395, ValA396, AsnA397, LysA403, LysB354, LysB371, ProB373, HisB374, SerB387, AsnB388, GlyB390, AlaB391, ArgB413, SerB416
Compound 5h	LysA403 arene-cation LysB371 arene-cation	ArgA344, AsnA362, TyrA377, PheA395, AsnA397, TyrA398, LysB354, LysB362, GlyB369, ProB373, HisB374, TyrB386, SerB387, AsnB388, IleB389, GlyB390, AlaB391, ArgB413
Compound 5i	HisB374 (2*)	ArgA344, GluA360, TyrA377, ValA394, PheA395, ValA396, AsnA397, TyrA398, LysA403, LysB354, ProB373, HisB374, SerB387, AsnB388, GlyB390, AlaB391, ArgB413, SerB416
Compound 5j	LysA403 arene-cation HisB374	ArgA344, TyrA377, ValA394, PheA395, ValA396, AsnA397, TyrA398, LysA403, LysB354, LysB371, ProB373, HisB374, AsnB388, GlyB390, AlaB391, SerB416

*; shows the number of hydrogen bonds

A simplified 2D binding interactions and 3D interactions of the two compounds with the highest affinity according to MOE docking (compound **5b** and **5d**) are given in Table 3. The two compounds have also exhibited the highest MIC value (0.8 $\mu\text{g/mL}$) among the synthesized imidazole derivatives. Compound **5d** has created a number of hydrogen bonding interactions with residues in the active site of GlmU^{Mtb}.


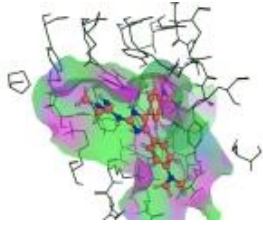
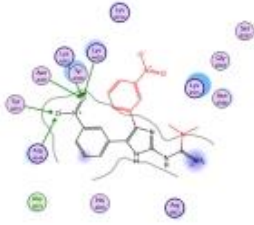
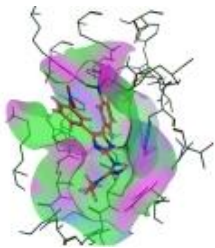
Ligands	Simplified 2D interactions	3D representation
Compound 5b		
Compound 5d		

Table 3: A 2D and 3D intermolecular interactions of the top two most active compounds during docking simulation.

In the 2D representation, the green circles show hydrophobic amino acids; the purple circles show polar amino acids; the blue regions on the ligand show regions exposed to solvent; the broken green arrow shows side chain acceptor; the broken blue arrow shows backbone donor.

Conclusions and Recommendations

All of the synthesized diaryl imidazole derivatives exhibited a promising anti-tubercular activity. Of all the synthesized compounds, compounds **5b-5e** were very interesting as they exhibited MIC value of 0.8 $\mu\text{g/mL}$. The substitution of the aromatic rings with groups capable of creating hydrogen bonding interactions was found to increase anti-tubercular activity. The use of difuranyl group in place of diphenyl group was found to preserve the activity of imidazole based anti-tubercular agents. A computationally guided structure based design of imidazole derivatives may lead to more potent inhibitors of the acetyl transfer reaction catalyzed by GlmU^{Mtb}.

Acknowledgments

The authors are grateful to MOE docking authorities and Sri Padmavathi School Of Pharmacy for providing the facilities to carry out this research work.

References

1. WHO. Global tuberculosis report 2021. World Health Organization, 26th edition. 2021
2. Velayati AA, Farnia P, Masjedi MR. The totally drug resistant TB. *Int J Clin Exp Med.* 2013;6:307–09

3. Dheda K, Migliori GB. The global rise of XDR-TB: Is the time to bring back Sanatoria now overdue? *Lancet*. 2012;379:773–75
4. Udwardia ZF, Amale RA, Ajbani KK, Rodrigues C. Totally drug-resistant TB in India. *Clin Infect Dis*. 2012;54:579–81
5. Udwardia ZF. Totally drug resistant-tuberculosis in India: The bad just got worse. *J Assoc Chest Physicians* 2016;4:41-2
6. Velayati AA, Masjedi MR, Farnia P, Tabarsi P, Ghanavi J, ZiaZarifi AH. Emergence of new forms of totally drug resistant TB bacilli: super extensively drug resistant TB or totally drug resistant strains in Iran. *CHEST J*. 2009;136:420–25
7. Anna AG, Garcia JL, Torrelles JB. Evolution of Drug-Resistant *Mycobacterium tuberculosis* Strains and Their Adaptation to the Human Lung Environment. *Front. Microbiol*, 2021;12:1-21
8. Shah NS, Richardson J, Moodley P, Babaria P, Ramtahal M, Heysell SK. Increasing drug resistance in XDR-TB, South Africa. *Emerging Infect Dis*. 2011;17:510–13
9. Seung KJ, Keshavjee S, Rich ML. Multidrug-Resistant Tuberculosis and Extensively Drug-Resistant Tuberculosis. *Cold Spring Harb Perspect Med*. 2015 Apr 27;5(9)
10. Zumla A, Nahid P, Cole ST. Advances in the development of new tuberculosis drugs and treatment regimens. *Nat Rev Drug Discov*. 2013;12:388-404
11. Zhang L, Peng X, Damu G, Geng R, Zhou C. Comprehensive review in current developments of imidazole based medicinal chemistry. *Med Res Rev*. 2014;34:340-437
12. Ali I, Lone MN, Aboul-Enein HY. Imidazoles as potential anticancer agents. *Medchemcomm*. 2017;13:8(9):1742-1773.
13. Siwach, A., Verma, P.K. Synthesis and therapeutic potential of imidazole containing compounds. *BMC Chemistry*. 2021;15:12
14. Iman M, Davood A, Dehqani G, Lotfinia M, Sardari S, Azerang P, Amini M. Design, synthesis and evaluation of anti-tubercular activity of novel dihydropyridine containing imidazole substituent. *Iran J Pharm Res*. 2015;14:1067-1075
15. Gupta P, Hameed S, Jain R. Ring-substituted imidazoles as a new class of anti-tuberculosis agents. *Eur J Med Chem*. 2004;39:805-814
16. Pandey J, Tiwari VK, Verma SS, Chaturvedi V, Bhatnagar S, Sinha S, Gaikwad AN, Tripathi RP. Synthesis and anti-tubercular screening of imidazole derivatives. *Eur J Med Chem*. 2009;44:3350-3355
17. Zampieri D, Mamolo MG, Vio L, Romano M, Skoko N, Baralle M, Pau V, De Logu A. Antimycobacterial activity of new N1-[1-[1-aryl-3-[4-(1H-imidazol-1-yl)-3-oxo]propyl]-pyridine-2-carboxamidrazone derivatives. *Bioorg Med Chem Lett*. 2016 [in press]
18. Zampieri D, Mamolo MG, Laurini E, Scialino E, Banfi E, Vio L. Antifungal and Antimycobacterial activity of 1-(3,5-diaryl-4,5-dihydro-1H-pyrazol-4-yl)-1H-imidazole derivatives. *Bioorg Med Chem*. 2008;15:4516-4522
19. Ginsberg AM, Laurenzi MW, Rouse DJ, Whitney KD, Spigelman MK. Safety, tolerability and pharmacokinetics of PA-824 in healthy subjects. *Antimicrob Agents Chemother*. 2009;53:3720-3725
20. Somasundaram S, Anand RS, Venkatesan P. *et al*. Bactericidal activity of PA-824 against *Mycobacterium tuberculosis* under anaerobic conditions and computational analysis of its novel analogues against mutant Ddn receptor. *BMC Microbiol*. 2013;13, 218
21. Kumarachari RK, Peta S, Surur AS, Mekonnen YT. Synthesis, characterization and in silico biological activity of some 2-(N,N-dimethyl guanidiny)-4,6-diaryl pyrimidines. *J Pharm Bioallied Sci*. 2016;8(3):181-7. doi: 10.4103/0975-7406.171678. PMID: 27413345; PMCID: PMC4929956.
22. Rajasekhar KK, Nizamuddin ND, Surur AS, Mekonnen YT. Synthesis, characterization, antitubercular and antibacterial activity, and molecular docking of 2, 3-disubstituted quinazolinone derivatives. *Res. Rep. Med. Chem*. 2016; 6: 15–26.
23. Jagtap PA, Soni V, Vithani N, Jhingan GD, Bais VS, Nandicoori VK, Prakash B. Substrate bound crystal structures reveal features unique to *Mtb* GlcNAc-1-P and a catalytic mechanism for acetyl transfer. *J Biol Chem*. 2012;287:39524-39537

24. Tran AT, Wen D, West NP, Baker EN, Britton WJ, Payne RJ. Inhibition studies on GlmU^{Mtb}. *Org Biomol Chem*. 2013;11:8113-8126
25. Singh M, Kempanna P, Bharatham K. Identification of Mtb GlmU Uridyltransferase Domain Inhibitors by Ligand-Based and Structure-Based Drug Design Approaches. *Molecules*. 2022;27(9):2805. doi: 10.3390/molecules27092805. PMID: 35566155; PMCID: PMC9105790.
26. Pereira MP, Blanchard JE, Murphy C, Roderick SL, Brown ED. High-throughput screening identifies novel inhibitors of the acetyltransferase activity of *Escherichia coli* GlmU. *Antimicrob Agents Chemother*. 2009;53:2306-2311
27. Mehra R, Rani C, Mahajan P, Vishwakarma RA, Khan IA, Nargotra A. Computationally guided identification of novel GlmU^{Mtb} inhibitory leads, their optimization, and *in vitro* validation. *ACS Comb Sci*. 2016;18:100-116
28. Franzblau SG, Witzig RS, Mclaughlin GC, Torres P, Madico G, Hernandez A, Degnan MT, Cook MB, Quenzer VK, Ferguson RM, Gilam RH: Rapid, low-technology MIC determination with clinical *Mtb* isolates by using the MABA. *J Clin Microbiol*. 1998;36:362-66
29. Velankar S, Alhroub Y, Alili A, Best C, Boutselakis HC. *et al* PDBe: Protein Data Bank in Europe. *Nucleic Acids Res*. 2011; 39: 402-10.
30. Lovell S, Davis I, Arendall III W, Bakker P, Word J, Prisant M, Richardson J, Richardson C. Structure validation by C α geometry: phi, psi and C β deviation. *Proteins*. 2002;50:437-50
31. Molecular operating environment (MOE), 2013.08; chemical computing group Inc., 1010 Sherbooke St. west, suite #910, Montreal, QC, Canada, H3A 2R7, 2015